

A Review of Brain Early Infarct Image Contrast Enhancement Using Various Histogram Equalization Techniques

Yu Jie Ng^a, Kok Swee Sim^{a,*}

^a Faculty of Engineering and Technology, Multimedia University, Jalan Ayer Keroh Lama, Bukit Beruang, Melaka, Malaysia
Corresponding author: *kssim@mmu.edu.my or sksbg2022@gmail.com

Abstract— Stroke is one of the leading causes of death worldwide, accounting for five of all deaths in Malaysia. It happens when an infarct from a blocked blood artery results in brain necrosis. Diagnoses involving brain diseases and injuries can be made with the help of CT scans, which create axial images by using exact X-ray measurements. These scans offer vital information on the anatomy and physiology of the brain. For an appropriate diagnosis, early infarct brain CT scan contrast can be improved. The two main types of histogram equalization (HE) approaches used for this purpose are Global Histogram Equalization (GHE) and Local Histogram Equalization (LHE), which is also referred to as adaptive histogram equalization (AHE). Locally, LHE uses the block overlapped method to improve photos. Additional sophisticated methods include Dualistic Sub Image Histogram Equalization (DSIHE), Contrast Limited Adaptive Histogram Equalization (CLAHE), Recursive Sub Image Histogram Equalization (RSIHE), Gamma Correction Adaptive Extreme Level Eliminating With Weighting Distribution (GCAELEWD), and Brightness Preserving Bi Histogram Equalization (BBHE). The contrast of brain images is greatly improved by these techniques. Nevertheless, a number of these methods have issues with blur, noise, and preserving local image brightness. According to our research, CLAHE and DSIHE are especially good to improve image contrast and yield better outcomes than other techniques. These methods lessen frequent problems, which makes them better suited to create precise and comprehensive brain images—an essential component of successful stroke diagnosis and treatment.

Keywords— Stroke; CT scans; histogram equalization; contrast enhancement; brain imaging.

Manuscript received 8 Dec. 2023; revised 18 Mar. 2024; accepted 12 Jul. 2024. Date of publication 31 Dec. 2024.
IJASEIT is licensed under a Creative Commons Attribution-Share Alike 4.0 International License.



I. INTRODUCTION

The brain has 100 billion neurons and 100 trillion connections, which weighs around 1300 grams. The left and right sections each have distinct purposes. The central nervous system (CNS), which controls routine movements, comprises the brain and spinal column. Brain issues can impact these crucial processes. Knowing the basic structure of the brain—which is made up of the brain stem, cerebellum, and cerebrum [1]—is essential to comprehending its anatomy [3], as shown in Fig. 1.



Fig. 1 Main components of brain [1]

The parietal lobe is in charge of touch, visual orientation, speech, hearing, and vision, whereas the frontal lobe controls emotions, speech, and bodily movements. Besides, the cerebellum, which is situated underneath the cerebrum, regulates bodily processes such as balance and coordination. The brain stem, which is connected to the cerebellum and spinal cord, controls vital functions including breathing and heart rate. The brain stem also sends signals to the body. Fig. 2 shows the brain images capture from MRI.

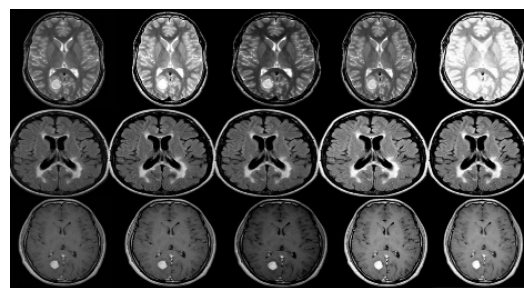


Fig. 2 Brain images captured from MRI [2]

In addition, the term "meninges" refers to the membranes around the brain and spinal cord. The meninges are composed of three layers: the dura mater, arachnoid mater, and pia mater. These covers accomplish two main goals. They protect the central nervous system (CNS) from mechanical damage and serve as a supporting structure for the cerebral and cranial arteries, along with cerebro-spinal fluid. Two major meningeal disorders that are frequently associated with meningitis are intracranial haemorrhages and meningitis. Fig. 3 depicts the relationships to the skull and brain.

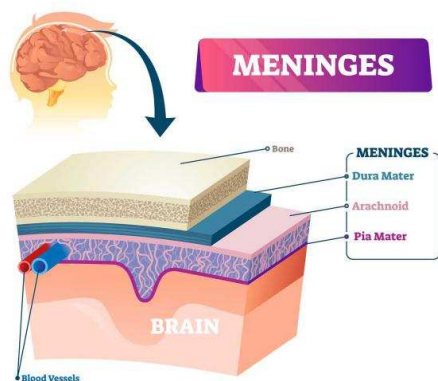


Fig. 3 The relationship between skull and brain [1]

A. Stroke Type

Internal brain damage is known as a stroke [11]. It indicates that there is a pause in or blockage in the blood supply. There are two primary causes of stroke. First, there is an abrupt stoppage or obstruction of the blood flow. It results in an irregular blood flow that does not nourish every portion of the brain. Second, there is an internal haemorrhage due to a damaged blood vessel. The internal bleeding will obstruct and impact the surrounding areas as well. Hemorrhagic is a type of stroke [4]. Our brains begin to malfunction when the blood supply is cut off and bursts, causing brain cells to die. We need to give this critical topic full attention. In addition, stroke is divided into other categories. The two most common types of strokes are hemorrhagic and ischemic, as seen in Fig. 4 and Fig. 5.

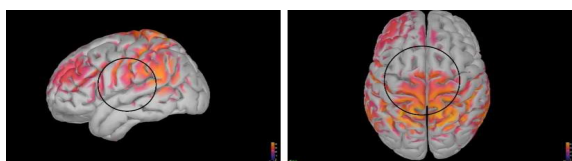


Fig. 4 Hemorrhagic stroke [5]

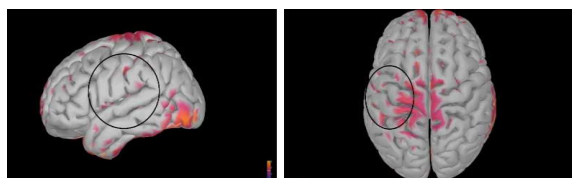


Fig. 5 Ischemic stroke [5], [7]

A blood vessel rupture or brain bleed may cause hemorrhagic stroke. Brain hemorrhages, also known as internal bleeding in the brain, can result from some diseases connected to blood vessels. Risk factors for hemorrhagic stroke are included in Table I.

TABLE I
RISK FACTORS AND PERCENTAGES [6],[7], [74]

Effect Size	Strength of Available Evidence		
	Strong	Moderate	Weak
Substantial (>100% Risk Modificati on)	<ul style="list-style-type: none"> Family History Race / Ethnicity APOE Gene Age Hypertension Alcohol Consumption Oral Anti-coagulation 	<ul style="list-style-type: none"> Sympathomimetic Drugs 	
	Modest (50-99% Risk Modificati on)	<ul style="list-style-type: none"> Body Mass Index (BMI) Anti-platelet Agents 	<ul style="list-style-type: none"> Cholesterol Levels Sleep Apnoea
Minimal (<50% Risk Modificati on)	<ul style="list-style-type: none"> SSRI Antidepressants 	<ul style="list-style-type: none"> 1q22 Locus COL4A1 Gene COL4A2 Gene 	<ul style="list-style-type: none"> Sex / Gender

One less frequent cause of bleeding in the brain is rupture of an arteriovenous malformation (AVM). An AVM is a randomly distributed, weakly-walled network of blood vessels. The most prevalent kind of strokes are ischemic strokes. It occurs when the blood arteries in the brain is blocked or narrowed. This leads to ischemia. Blood vessels may become narrowed or clogged due to fatty deposits building up in the arteries. On the other hand, they might be caused by material or blood clots that travel through the blood vessels, generally from the heart. An ischemic stroke may result from debris, blood clots, or fat deposits being lodged in the brain's blood vessels. A blood clot commonly happens when plaque builds up in the arteries, a disease known as atherosclerosis. In addition to the carotid artery in the neck, it can occur in other arteries [5],[8]. Table II shows the characteristics of ischemic stroke and hemorrhagic stroke.

TABLE II
CHARACTERISTICS OF ISCHEMIC STROKE AND HEMORRHAGIC STROKE [6],[7]

	Ischemic Stroke	Hemorrhagic Stroke
Pathogen	<ul style="list-style-type: none"> Blood flow is cut off, which leads to Ischemia BLOCKAGE Thrombosis: A blood clot has formed on the wall of the vessel 	<ul style="list-style-type: none"> The collection of blood in the brain leads to Ischemia & increased ICP BLEEDING
Causes	<ul style="list-style-type: none"> Embolism: Piece of a blood clot, foreign body, or air/bodily fluid occludes a vessel 	<ul style="list-style-type: none"> Ruptured artery Aneurysm (weakening of the vessel) Uncontrolled hypertension
Treatment	<ul style="list-style-type: none"> Fibrinolytic therapy (CLOT BUSTERS) 	<ul style="list-style-type: none"> Stop the bleeding Prevent Increased ICP

B. Signs and Symptoms

Since ischemic strokes are the most prevalent, we shall concentrate more on them in this paper. Additionally, stroke

is not precluded from having its symptoms, particularly in the case of a transient ischemic attack (TIA) [9]. Unlike other strokes, the blood clot develops and stops the blood flow relatively quickly, sometimes lasting only a few minutes. Therefore, the indicators are the most crucial.

To raise the public awareness of stroke warning signs, the American Heart Association, the National Stroke Association, and other organizations have adopted the acronym FAST, which stands for facial drooping, arm weakness, speech difficulty, and time. In 1998, FAST was initially made accessible in the UK. However, two more critical stroke symptom signals are now included in the new acronym FASTER, created by Beaumont Health's stroke specialists. The new meaning of the term is shown in Fig. 6 [10].

Know the Symptoms of a Stroke

Early recognition is the key to proper stroke treatment.
Thinking **FASTER** might help you save a life.

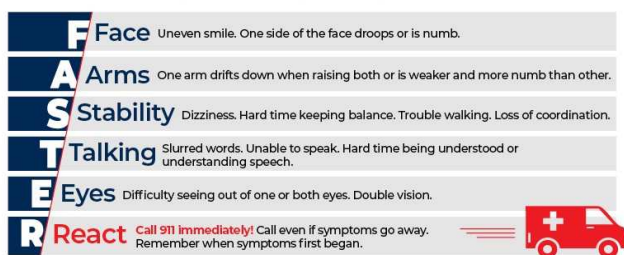


Fig. 6 Acronym “FASTER” descriptions [10]

According to Rebecca Grysiewicz, D.O., head of the Comprehensive Stroke Centre at Beaumont Hospital in Royal Oak, a new concept called FASTER highlights the importance of recognizing stroke symptoms and calling 911 as soon as possible [10]. When we designed FASTER, Beaumont included "eyes" and "stability" since sudden imbalance and loss of vision are also significant and distinct symptoms of a stroke. To evaluate potential stroke therapies, timely hospital admission requires timely symptom diagnosis and fast response.

C. Diagnosis Method of Brain Lesion

As seen in Fig. 7, the computed tomography scan (CT scan) creates a succession of two-dimensional cross-sectional brain images using an x-ray beam and a computer interface. It is a non-invasive, safe procedure. A CT scan can identify strokes as well as tumors. Ischemia and infarction may not be readily seen on a CT scan during the first 24 hours. Certain infarcts are also difficult to observe on CT scan imaging, even 48 hours later. It is an effective technique for identifying internal brain hemorrhage. Because it scans, it is very frequently used in emergencies. Thus, the paper makes use of a CT scan [16], [46], [72].

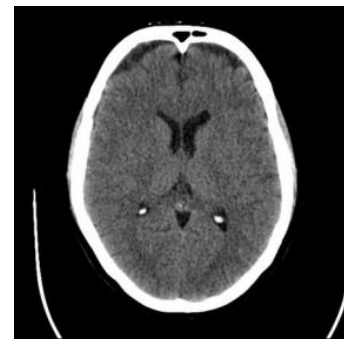


Fig. 7 CT brain image [12]

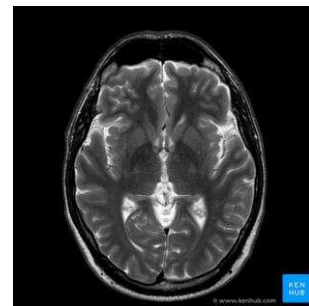


Fig. 8 MRI brain image [13]

A safe, non-invasive method for studying the brain, magnetic resonance imaging (MRI) uses radio frequency radiation and a magnetic field. Although it is a costly procedure, it provides various brain image dimensions. Fig. 8 shows the example of MRI Brain Image [16], [37], [61], [72].

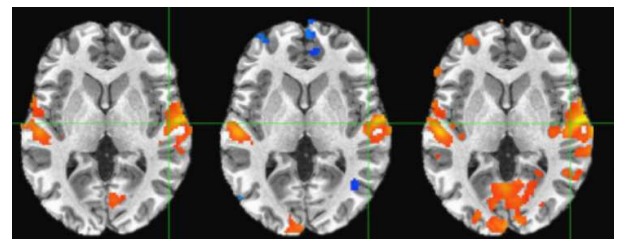


Fig. 9 fMRI brain image [14]

As shown in Fig. 9, functional magnetic resonance imaging (fMRI) provides a functional image of the brain and can identify variations in blood flow.

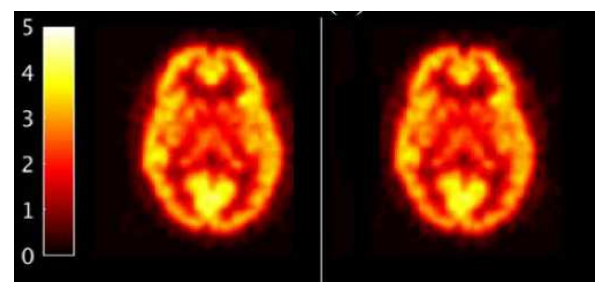


Fig. 10 PET brain image [15]

Peptide-tron emission tomography (PET) creates brain images by detecting radioactive materials injected into the brain. The costly procedure entails gamma ray recording. Figure 10 shows an example of a PET Brain Image [66].

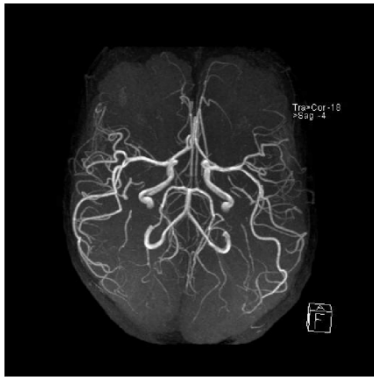


Fig. 11 Angiography brain image [17]

A technique called angiography involves injecting dye into the blood, waiting for it to pass through the brain, and then using X-rays to identify images of blood vessels. As shown in Fig.11, Table III shows the advantages and limitations of CT, MRI, and PET.

TABLE III
ADVANTAGES AND LIMITATIONS OF CT, MRI, AND PET

	Advantages	Limitations
CT	<ul style="list-style-type: none"> Anatomy Spatial resolution (1mm) Fast acquisition 	<ul style="list-style-type: none"> Irradiating Contrast Artifacts (metal, teeth, etc)
MRI	<ul style="list-style-type: none"> Anatomy and function Spatial resolution (1mm) Contrast (soft tissue) Non-irradiating 	<ul style="list-style-type: none"> Long acquisition Compatible MRI equipment with high-performance dedicated coils Contraindications Artifacts (Distortions, no uniformity, etc)
PET	<ul style="list-style-type: none"> Function Tumor/Background Contrast Acquisition field 	<ul style="list-style-type: none"> Irradiating Spatial resolution (>3/4mm) Partial volume (blurred edges)

D. Non-contrast computed tomography (NCCT)

Typically, radiologists utilize NCCT to identify early signs of infarction and notify the physician. It can assist the patient in making the most of the infarction treatment window [32]. However, because of the subtlety of the stroke and the image quality, it is challenging to locate the stroke. [18] The medical community now struggles with consensus and precision when identifying early CT scan changes. As a result, radiologist and physician experiences are crucial. Rather than providing them with training, the NCCT image's contrast enhancement techniques are essential in assisting physicians and radiologists in quickly identifying the infarction [67], [71].

E. Hounsfield Unit and Windowing

This paper addresses the CT brain scan, emphasizing its fundamental components and interpretation, proposing that the scanned image's left side corresponds to the right side. Using the Hounsfield Unit (HU) scale, CT scans display grey levels depending on radiation attenuation that are separated into tissue densities (air and bone). The grey-level display gets darker as the HU decreases [29]. Fig. 12 shows the range of HU. Fig. 13 shows an example of CT Brain ranges in HU.

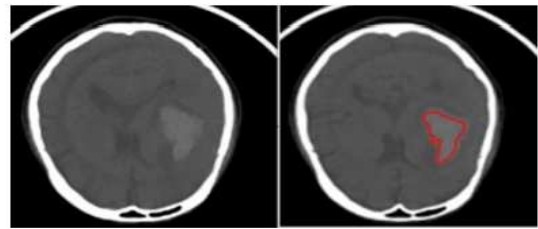


Fig. 12 Brain Hemorrhage segmentation based on HU values [19]

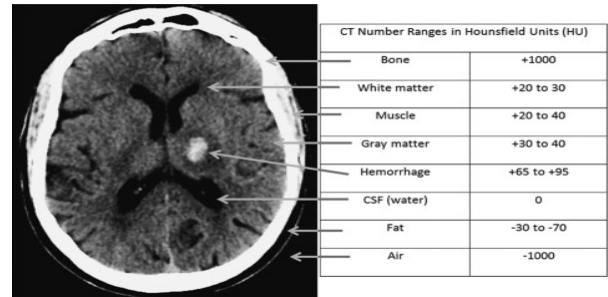


Fig. 13 Example of CT brain ranges in HU [19]

Furthermore, windowing in a CT brain image is important. The window setting aids in the detection of pathologies involving the skull, brain tissue, and other materials. It is separated into window level (WL) and window width (WW). While the HU in the middle of the WW is WL, the range of HU that shown is WW. As a result, various window settings will show different brain regions. Fig. 14 and Table IV are the sample for default window setting [45].

TABLE IV
SAMPLE OF DEFAULT WINDOW SETTING

	Window Width (WW)	Window Level (WL)
Brain	80	40
Bone	2500	480
Subdural	350	90

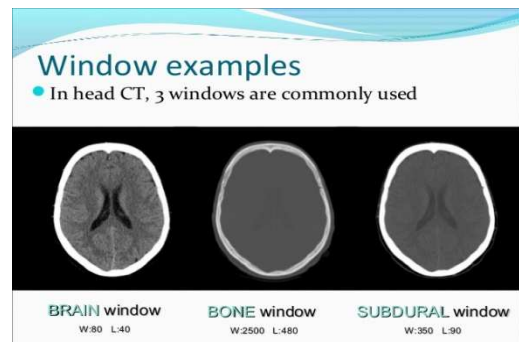


Fig. 14 Window example [20]

F. Medical Image File Format

Two categories can be used to categorize medical image file formats. The first is a format called DICOM [4] that aims to standardize the images produced by diagnostic modalities. The secondary collection of formats aims to enhance and streamline post-processing analysis. Among these formats are Analyse [5], Nifti [6], and Minc [7]. DICOM format is frequently used to store medical image files. The metadata and image data are combined into a single file and stored at the start of the file. The DICOM, Minc, and Nifti file formats employ this paradigm. In the second setup, one file contains

the photo data, while another contains the information. The Analyse file format (.hdr and .img) uses the two-files paradigm. The table of descriptions for the various formats is displayed in Table V.

TABLE V
SAMPLE DIFFERENT FILE FORMAT CHARACTERISTICS

Summary of file formats characteristics			
Format	Header	Extension	Data Types
Analyze	Fixed-length: binary format with 348 bytes	.img and .hdr	Eight-bit unsigned integers, 16- and 32-bit signed integers, 32- and 64-bit floats, and 64-bit complexes
Nifti	Fixed-length: 352 bytes in binary format (or 34 bytes for data saved in .img and .hdr formats).	.nii	Float (from 32 to 128 bits), signed and unsigned integer (from 8 to 64 bits), and complex (from 64 to 256 bits)
Minc	Broad binary format	.mnc	Float (32, 64 bits), complex (32, 64 bits), signed and unsigned integer (from 8 to 32 bits)
DICOM	Variable length binary format	.dcm	Integer (8-, 16-bit; 32-bit only permitted for radiation dosage) that is signed and unsigned; float not supported

II. MATERIALS AND METHODS

These days, contrast enhancement is crucial and helpful for medical imaging, particularly brain images [73]. We cannot comprehensively analyze the CT Scan image because of the obtained image's low contrast and noise. Therefore, we need to use contrast enhancement techniques to solve the issue that radiologists and doctors face [29], [30]. It may aid in accelerating and improving the accuracy of the stroke diagnosis. The methods now used to enhance the contrast of CT brain images are HE, AHE, BBHE, DIHE, GCAELEWD, and others.

A. Histogram Equalization (HE)

Histogram equalization techniques (HE) are widely used in image processing to improve contrast. Adjusting the image's pixel value distributes the grayscale values as uniformly as possible [5]. Stated differently, the HE method aims to generate better contrast by spreading out the input intensity levels throughout the whole range of values. The results of the histogram both before and after the HE approach is used are displayed in Fig. 15. Global Histogram Equalization (GHE) and Local Histogram Equalization (LHE) are the two basic approaches that make up HE techniques [4].

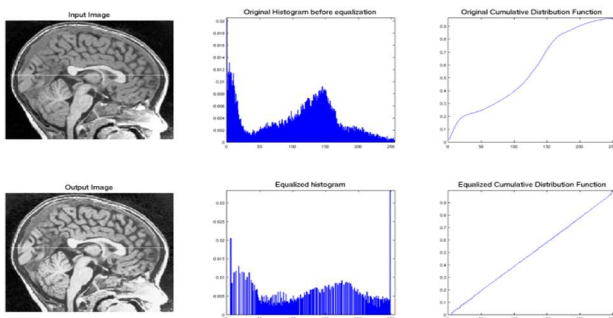


Fig. 15 Histogram before and after equalization

To estimate the gray level intensity of an inserted image, the GHE approach employs global histogram information to produce a complete histogram. This image is then modified using the Probability Density Function (PDF) ($p(I_k) = \frac{h(I_k)}{\text{size of image}}$) and Cumulative Density Function (CDF) ($c(I_k) = \sum_{j=0}^k p(I_j)$). When employing lower-frequency gray levels, the GHE approach improves contrast in images but may lose contrast in high-frequency regions. Due to this restriction, it is best suited for general improvement; it can make embedded images more contrasty.

B. Adaptive Histogram Equalization (AHE)

Adaptive Histogram Equalization (AHE) is also known as Local Histogram Equalization (LHE). [14] [15]. Both standard and medical images exhibit substantial contrast enhancement when using this approach. AHE is superior in window setting compared with other image class methods; it improves images automatically and consistently [16]. The application of the AHE approach helps to get over GHE's limitations. This method does the local augmentation using the block-overlapped approach. The stages involved in the AHE method are shown in Fig. 16 [5].

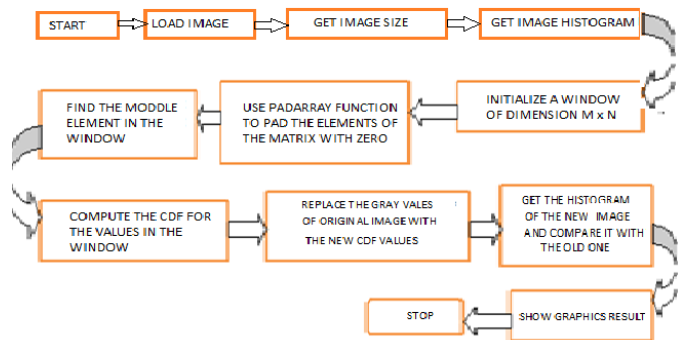


Fig. 16 Proposed algorithm on AHE [5]

As the research paper is summarized, the GHE approach can resolve the AHE restriction. However, certain areas of the image will have too many details. In addition, it struggles with increasing noise, and the computational process is expensive and sluggish [17].

C. Brightness Preserving Bi Histogram Equalization (BBHE)

The brightness of the embedded image may be controlled using the brightness-preserving histogram Equalization (BBHE) approach, which is based on histogram equalization [5]. The imported image is divided into two areas. One zone is separated where it is greater than the mean value, while another part is separated neither over nor equal to the mean value of the inserted image. The two zones are divided based on the inserted image's mean value. The PDF and CDF are then used as transfer functions to equalize the histograms of the two areas independently. Then, the two equalized histograms are integrated to obtain a brightness-preserving outcome. The entire BBHE method procedure is shown in Fig. 17. Depending on the mean value, the BBHE approach can maintain the brightness of the inserted image. However, this procedure has another issue that would impact the histogram's grayscale distribution level.

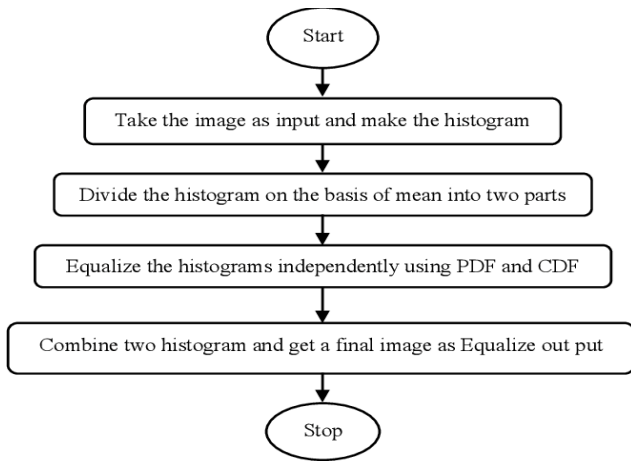


Fig. 17 Block diagram of BBHE technique procedures

D. Dualistic Sub Image Histogram Equalization (DSIHE)

Dualistic Sub Image Histogram Equalization (DSHE) is another histogram equalization-based approach that shares similarities with the BBHE technique [5]. It keeps the input brightness constant [56] and divides the inserted image into two areas. However, the median value is used to divide the two zones. One area is divided not more than or equal to the inserted image's median value, while another part is divided more than the median value [68].

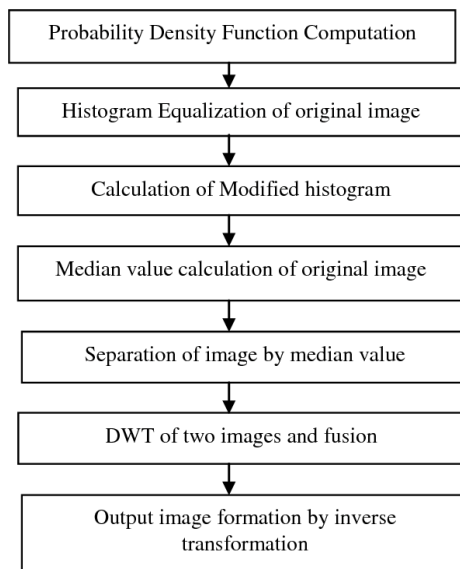


Fig. 18 Block diagram of DSIHE technique procedures

The PDF and CDF are then used as transform functions to equalize the histograms of the two areas independently. $(c_{lower\ region}(I_k) = \frac{1}{p} \sum_{i=0}^k pi)$ and $(c_{upper\ region}(I_k) = \frac{1}{p-1} \sum_{i=m}^{lower-1} pi)$ display the two transform functions, respectively (where k is the intensity value; m is the median value, and lower is the lower region value). Then, the two equalized histograms are integrated to obtain a brightness-preserving outcome. Fig. 18 illustrates the DSIHE technique's process flow. Like the BBHE method, DSIHE can preserve image brightness only by the median. Additionally, it creates an issue that will influence the histogram's degree of grey distribution.

E. Contrast Limited Adaptive Histogram Equalization (CLAHE)

The Contrast Limited Adaptive Histogram Equalization (CLAHE) methodology is a spatial domain method that is explored [70]. This approach helps to boost contrast when there is a vital necessity for brightness in the image. The highest entropy will be employed to get the best histogram equalization, and the contrast of the input image will be restricted. The image is divided into similar regions using the CLAHE approach, and each area is then equalized [18]. As a result, the gray level distribution will become more uniform. The input image's invisible portion will be more visible [31], [60].

The following are the CLAHE method steps. Initially, the inserted image is divided into a square section eight times 8. The non-overlapping contextual sections are all these eight times eight square areas. Secondly, each part's intensity histogram is computed individually. Third, the histogram's clipping limit is established. The local image region's contrast will decrease when the clipping limit is lowered. Therefore, we must adjust it to the most favorable minimal value. Fourth, each histogram's transform function is chosen for modification. Fifth, $(G = [g_{max} - g_{min}] \times p(f) + g_{min})$ is applied to each histogram where G is the computed pixel value, g_{min} = minimum value of pixel, g_{max} = maximum value of pixel and $p(f)$ is the Cumulative Probability Distribution (CPD). Sixth, all the components are combined using bi-linear interpolation.

F. Recursive Sub Image Histogram Equalization (RSIHE)

The input image is segmented recursively using maximum entropy separation using the Recursive Sub image Histogram Equalization (RSIHE) approach [19]. The imported image is divided into several sub-images [57]. (Number of sub images = 2^l) is applied to divide the embedded image into subimages [20], where l is the iteration number.

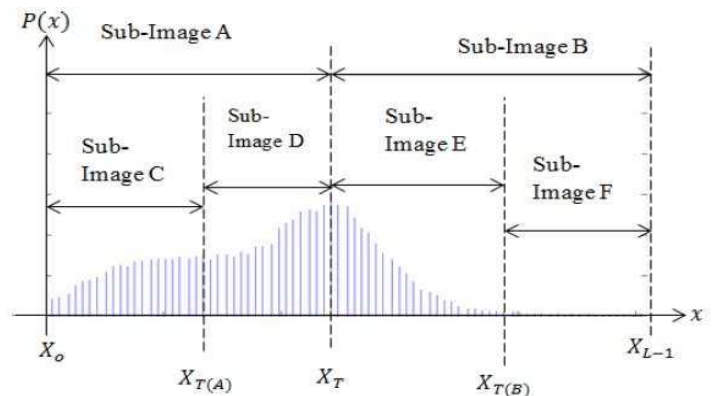


Fig. 19 Segmentation of RSIHE approach with an iteration of two

Fig. 19 shows the segmentation of this approach with an iteration of two. The sub-images A and B from Fig. 19 are separated from the histogram. The sub-histogram of sub-image A is used to determine the threshold value $X_{T(A)}$. The threshold value has also been discovered for sub-image B. The maximal entropy computation is then used to determine the X_T . The iteration's value of 2 will produce four sub-images: C, D, E, and F.

This approach uses sub-image processing based on the GHE technique to help alleviate the weakness in the histogram equalization. RSHE can lessen the undesired artifacts. Additionally, it makes the violation more contrasted and somewhat brighter than the brain's normal tissue. However, this method will muddy the outcome.

G. Gamma Correction, Adaptive Extreme Level, Eliminating with Weighting Distribution (GCAELEWD)

The Gamma Correction Adaptive Extreme Level Eliminating with Weighting Distribution (GCAELEWD) approach is covered in this study. This technique involves altering the histogram. It has been altered under the GHE method. To address these drawbacks with the previous approaches, GCAELEWD was developed. Fig. 20 shows how this strategy works [21], [25]:

Equation $(PDF(I_{l_s}) = \frac{n_{l_s}}{n}, \text{ for } l_s = 0, 1, \dots, L - 2)$ is used to eliminate two extreme levels in order to execute the first subtitle. Equation $(PDF_{WDF}(I_{l_s}) = PDF_{max_s} (\frac{PDF(M_{l_s}) - PDF_{max_s}}{PDF_{max_s} - PDF_{min_s}})^\alpha)$ is created as the new PDF.

Equation $(CDF_{WDF}(M_{l_s}) = \sum_{l_s=1}^{l_a} PDF_{WDF}(I_{l_s}))$ is used to calculate CDF, which is then normalized into [0, 1]. Equation $(TF_{GCAELEWD}(I_{l_s}) = \frac{CDF_{WDF}(I_{l_s}) + I_{l_s}^{1 - CDF_n(I_{l_s})}}{2})$ is used to calculate the transfer function, and the resultant value is stored in the array Nil.

The resulting image is then blended using the bilinear interpolation technique. This technique combines the image to roughly represent each pixel's ideal value. When all of the tiles are combined, it might lessen the irregular line. Each split tile, for instance, is further divided into four tiny square tiles. Fig. 21 shows how the transform function of the first subtitle is transferred using dark gray pixels at the borders. Next, the pixels in the border section with a lighter color are subjected to linear interpolation. However, the white pixels in the center are used for the bi-linear interpolation approach. Consequently, the GCAELEWD approach can preserve the added image's brightness change and improve the brain image's quality.

H. Extraction Method

Extracting a brain lesion from a CT scan image was explained. It begins with the identification. The lesion will be automatically detected by measuring the volume. Due to differences in tissue densities in the input image, the histogram's intensity of color analysis is used to assess the lesion's level [22]. This evaluation is recommended using the segmentation level in the image processing stage. A mask will be applied to the captured image after the pre-processing stage. We will retrieve the divided level. The area of the lesion will be automatically calculated when the mask has been placed. It is crucial because the second step quantifies and computes the lesion's volume. As seen in Fig. 22, the area versus length graph is displayed. Equation $(S = \int_a^b f(x) dx)$ is used to get the lesion's volume. The area under the graph, S is calculated using this equation $(S = \int_a^b f(x) dx)$.

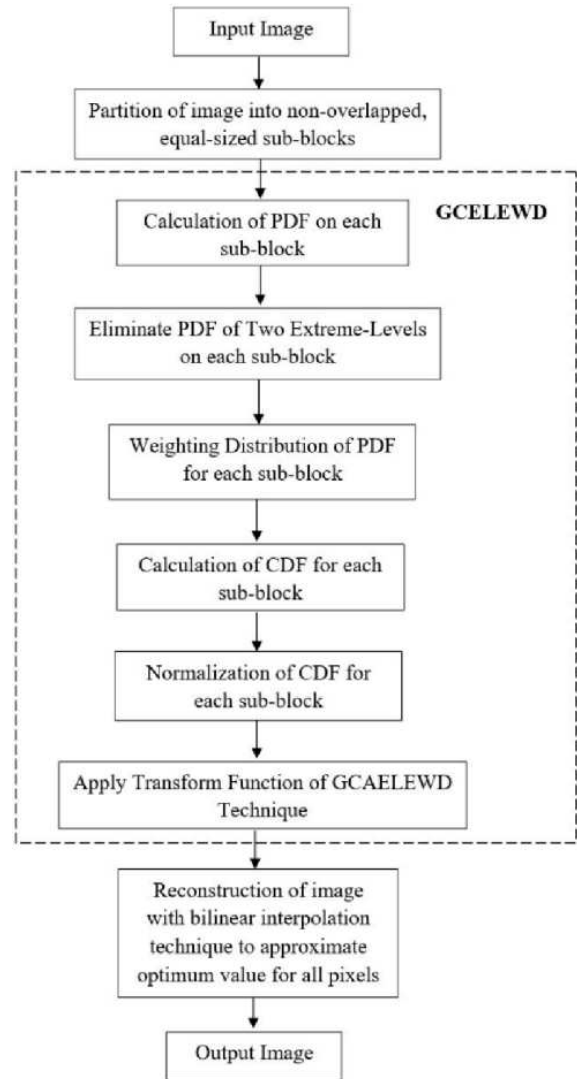


Fig. 20 GCAELEWD technique procedure

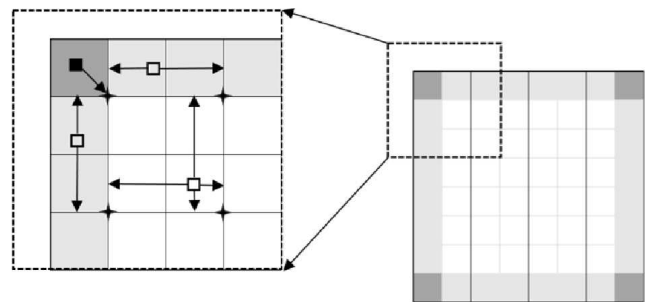


Fig. 21 Bi-linear interpolation technique

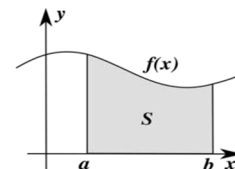


Fig. 22 Predicted graph

A clever strategy is applied to fragment the lesion. The most popular and practical edge detector for segmentation is the Canny approach. The intelligent detection approach consists of three easy stages. First, noise is removed using the

median approach. The gradient computation comes next. Last but not least is following the edge.

The lesion is then extracted using the sub-matrix operation in the cropping procedure. Two edges are chosen to create a rectangle around the lesion area, then cropped out. A binary image with an appropriate threshold value is made from the cropped image. Thus, the lesion has been effectively removed. Fig. 23 depicts the extraction procedure in its entirety.

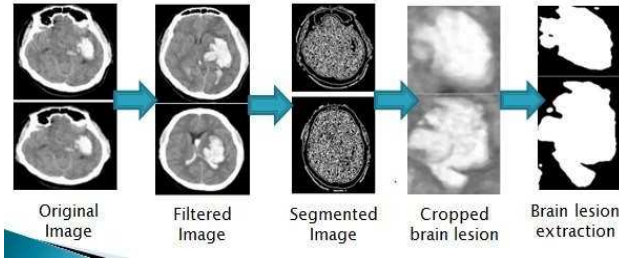


Fig. 23 Brain lesion extraction process

This segmentation approach has the benefit of automatically calculating the lesion's volume, eliminating the need to measure each lesion individually. Nonetheless, this segmentation method still has weaknesses. Measuring and computing are just the estimated areas for the associated masking level. As stated otherwise, the masking level should be virtually marked in the image while calculating the area. The entire procedure will be correct if the lesion is located correctly.

This approach is significantly more straightforward for a brain CT scan image. Since the MRI brain image is the focus of other lesion extraction. Additionally, compared to a CT scan, an MRI brain image has a far higher resolution. Therefore, the lesion may be extracted from a CT brain image using the described extraction approach. Related work in early infarct brain detection covers imaging techniques, biomarker and blood tests, artificial intelligence and machine learning, mobile health and telemedicine, EEG, EMG and ECG, and cancer. We can address based on imaging techniques, biomarker blood tests, artificial intelligence and machine learning, mobile health and telemedicine, EEG, EMG and ECG, and cancer.

Image techniques cover Computed Tomography (CT scans) and a) Magnetic Resonance Imaging (MRI). Non-contrast CT is frequently the first imaging modality to detect early indications of ischemia and Hemorrhagic stroke. CT Angiography enables the identification of blockages to provide comprehensive views of blood vessels. Magnetic resonance imaging (MRI) is extremely sensitive in identifying regions of limited water diffusion following ischemia injury. This is a sign of early brain infarcts [37]. Perfusion MRI evaluates cerebral blood flow to detect areas that are at risk, but this approach has yet to experience an infarction.

The quest remains for particular blood biomarkers that may signal an early brain infarct. These biomarkers offer a rapid and noninvasive way to detect them. Artificial intelligence (AI) and machine learning algorithms are being developed to evaluate imaging data and clinical information and detect brain infarcts early on. The goal of these technologies is to improve diagnosis speed and accuracy. For image analysis, AI systems can identify minute alterations in brain imaging that may be suggestive of early infarcts [23], [24], [28],[36], [42], [62].

Predictive Modeling is based on patient data and machine learning models. It can forecast the risk of stroke, which could notify medical professionals to take preventive action. Image colorization is another technique to highlight the area of early infarction [27], [49]. Patients at risk of stroke are being monitored using mobile health apps and telemedicine platforms. These platforms give healthcare professionals access to real-time data and facilitate quick action in the event of an early stroke indication.

Early infarct detection is crucial for effective treatment and improved outcomes. Electroencephalogram (EEG), Electromyogram (EMG), and Electrocardiogram (ECG) are three tools that can provide valuable information in different medical scenarios [26], [33]. We can also develop augmented and virtual rehabilitation and attentive learning with EEG, EMG, and ECG [35], [43], [44], [55], [64]. Cancer may not directly cause an infarct, but the associated risk factors, such as hypercoagulable states, treatment effects, and paraneoplastic syndromes, can cause the risk of strokes and myocardial infarctions [63]. Understanding these relationships, comprehensive management strategies can help reduce and improve cancer patient outcomes [65], [75].

III. RESULTS AND DISCUSSION

The GCELEWD approach was compared with BBHE, CLAHE, RSIHE, and DSIHE procedures to assess the performance of enhanced CT brain images. A dataset of 300 non-contrast CT brain images gathered from hospitals was used to evaluate the methods. Figs. 24 to 27 display enhanced CT brain images created using different techniques. The two primary areas of performance evaluation are qualitative and quantitative testing.

During the qualitative assessment, the complete augmented image is observed and perceived. It is stated differently to assess clarity and distinguish between normal and diseased tissue using our unaided sight. However, quantitative testing uses metrics like Mean-Square Error (MSE), [50], [54], Peak Signal-to-Noise Ratio (PSNR), and Structural Similarity Index (SSIM) [51]. Table VI compares MSE, PSNR [55], and SSIM with different categories of stroke.

TABLE VI
COMPARISON OF MSE, PSNR, AND SSIM WITH DIFFERENT CATEGORIES OF STROKE

	BBHE	RSIHE	GCELEWD	CLAHE	DSIHE
Average MSE					
Isch.	2400.95	698.75	528.17	349.25	629.01
Hemor.	1846.85	593.07	565.21	206.31	485.57
Average PSNR					
Isch.	13.33	19.70	21.75	22.75	20.16
Hemor.	15.44	20.41	20.69	24.98	21.41
Average SSIM					
Isch.	0.4660	0.9027	0.8258	0.6573	0.9043
Hemor.	0.3806	0.8800	0.5165	0.5870	0.9041

From Fig. 24 - 27, it is evident that the original background brightness was not preserved by the BBHE method. Images improved with the BBHE techniques have a brighter backdrop. Additionally, the contrast of the CLAHE approach is nearly identical to that of the original image. In certain instances, it cannot distinguish significantly between the usual brain soft tissue and ROI. The DSIHE technique brightens the normal brain tissue while intensifying the infarction's contrast. It has

the potential to lessen the production of undesired artifacts. On the other hand, the chosen NCCT brain image is blurred.

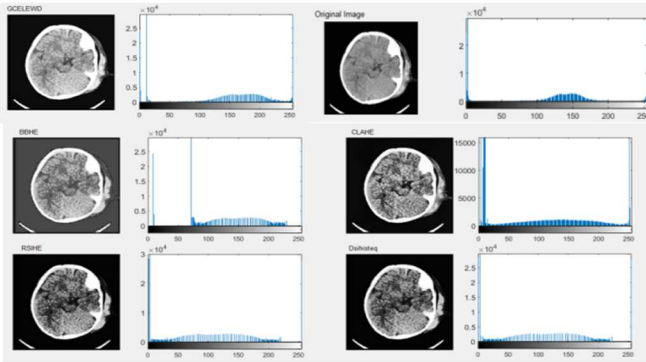


Fig. 24 Comparison of different histogram techniques of Ischemic stroke image 1

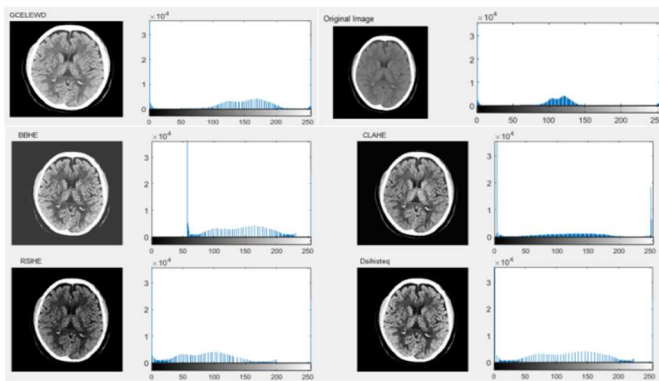


Fig. 25 Comparison of different histogram techniques of ischemic stroke image 2

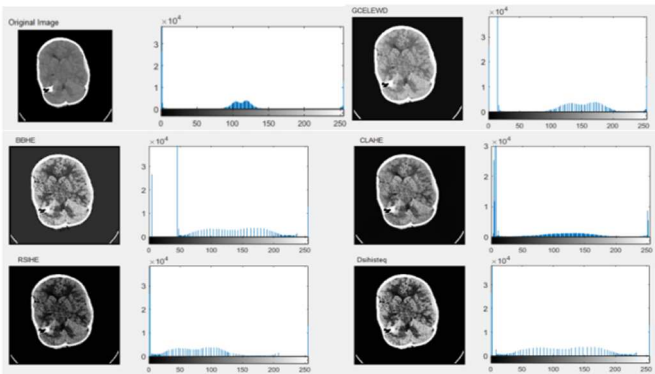


Fig. 26 Comparison of different histogram techniques of hemorrhagic stroke image 1

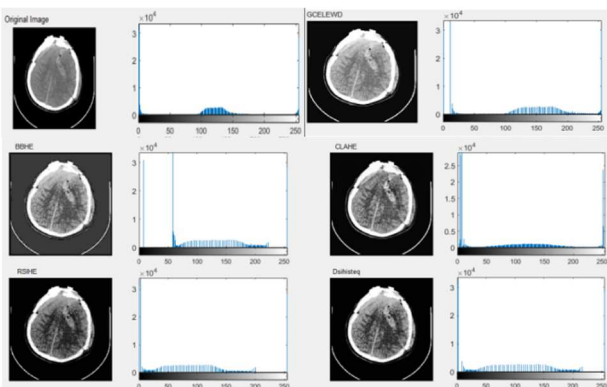


Fig. 27 Comparison of different histogram techniques of hemorrhagic stroke image 2

From Table VI, the CLAHE technique has the lowest Mean Square Error (MSE), followed by GCELEWD, DSIHE, RSIHE, and BBHE. Moreover, the CLAHE technique has the highest Peak Signal Noise Ratio (PSNR), followed by DSIHE, GCELEWD, RSIHE, and BBHE. While for the Structural Similarity Index (SSIM), DSIHE has the highest value, followed by RSIHE, CLAHE, GCELEWD, and BBHE. MSE is employed to evaluate how estimates or projections correspond with actual values. The closer the forecast is to reality, the lower the MSE. The ratio of the strongest signal to the noise level, expressed in decibels, is called PSNR. A low PSNR score suggests more noise or distortion in the processed image than in the original. However, there is a way to gauge how similar two images are: the Structural Similarity (SSIM) index. The SSIM values are 0 to 1, where 1 denotes a perfect match between the original and rebuilt images. Generally speaking, promising quantity reconstruction approaches have SSIM values of 0.97, 0.98, and 0.99. Thus, CLAHE and DSIHE are better at image enhancement [69].

In summary, the Histogram Equalization (HE) approach is well-liked due to its simplicity of use and quick processing time [38],[39]. Nevertheless, this method has some disadvantages, including noise addition, increased background contrast, and signal distortion [74]. Because the gray levels are stretched throughout the whole gray level range, the HE may result in saturation artifacts and over-enhancement results. Furthermore, many HE kinds rely on the global approach. Nevertheless, it is discovered that these global image processing strategies are inadequate to combat variations brought on by changes in light, such as morphologic and image clustering [47], [48]. Handling variance in non-uniform illumination with these global processing algorithms is still challenging.

A popular method for enhancing contrast in medical imaging, such as brain scans for early infarct diagnosis, is histogram equalization, or HE [40]. Nevertheless, there are some difficulties in applying HE in this situation and possible solutions to these difficulties. We can divide them into challenges and improvements.

A. Challenges

The challenges cover noise amplification, loss of details, the global nature of HE, artifact introduction, and non-uniform illumination. All these challenges have their issues and impacts, and they are discussed as noise amplification, loss of details, and the global nature of HE. For noise amplification, the noise is introduced by histogram equalization, which can exacerbate the problem of distinguishing true infarct zones from noise. This may obfuscate crucial information or result in false positives. About the loss of detail, HE can occasionally result in over-enhancement, which erases little but significant information from the image. Diagnostic accuracy may suffer from the loss of minute features essential for the early identification of infarcts [76].

For the global nature of HE, standard HE may not be appropriate for medical images with variable local contrast because it applies the same alteration to the entire image. Low contrast areas might need to be adequately enhanced while other areas might be too improved. In artifacts, photos are with huge uniform areas or areas with varied intensity

distributions. HE might introduce artifacts. Artifacts can complicate diagnosis and increase the difficulty of interpretation. In medical imaging, particularly brain images, non-uniform lighting is a common problem that HE can worsen. This may cause some imaging regions to be incorrectly interpreted as healthy or infarcted.

B. Possible Improvements

Improvements cover adaptive histogram equalization, contrast-limited adaptive histogram equalization, multi-scale histogram equalization, histogram matching, hybrid models, machine learning, and AI technologies. We can divide improvements into solutions, benefits, and considerations. Adaptive histogram equalization (AHE) applies histogram equalization to the full image, focusing more on specific areas (tiles) of the image. In terms of benefits, it can minimize the possibility of noise amplification and detail loss while enhancing local contrast. For consideration, the borders of these areas need to be blended carefully to prevent the introduction of artifacts.

For contrast-limited adaptive histogram equalization (CLAHE), noise amplification can be reduced by restricting contrast amplification. For the benefit, it can retain visual information and avoid over-enhancement. For the implementation, we can improve local contrast while preserving overall image quality [51], [52] in medical imaging software. For the multi-scale histogram equalization [58], we can use histogram equalization across a range of resolutions or scales. In terms of benefit, it enhances balance by improving small details and more considerable contrast differences. We can integrate outcomes from many scales to enhance the approach's image. Histogram matching helps with the equalization process and uses a reference histogram created using sharply contrasted images of infarct regions known to be healthy [34]. In terms of benefit, it gives the image the contrast that is helpful for diagnosis. The application aids in harmonizing contrast enhancement procedures across various scanners and photographs.

The hybrid method combines HE with other image enhancement techniques [53], such as those based on ML, edge detection, and smoothing filters. In terms of benefits, it preserves significant diagnostic qualities while addressing the constraints of HE. Combining Gaussian smoothing with CLAHE can then boost contrast and minimize noise. In machine learning and AI techniques, we can learn the best contrast enhancement parameters using deep learning models based on vast datasets of labeled brain images [59]. In terms of benefit, it can offer context-aware improvement tailored to the unique characteristics of early infarcts. For the implementation, we can ensure good generalization across various patient groups and imaging settings; models are trained on multiple datasets.

Histogram equalization is a helpful method for improving the contrast of brain images, particularly for the early diagnosis of infarcts. However, this technique has a few drawbacks, including noise amplification, loss of clarity, and its universal use. These difficulties can be overcome using adaptive strategies like CLAHE, multi-scale approaches, histogram matching, hybrid methods, and cutting-edge AI algorithms [41]. This will improve diagnostic results and increase the precision of early brain infarct identification.

IV. CONCLUSION

This overview examines the history of brain lesions known as strokes, focusing on the use of computed tomography (CT) scans for diagnosis. CT scans are employed due to their ability to quickly and accurately identify internal brain hemorrhages. The Digital Imaging and Communications in Medicine (DICOM) format stores CT brain images. Non-contrast CT brain imaging has lower diagnostic accuracy, necessitating contrast enhancement techniques to improve image quality. The Hounsfield unit scale is crucial for analyzing CT brain images, as it enables the visibility of internal brain tissue. Windowing techniques are used to observe various tissue densities in the brain image. Image enhancement, a key sub-field of digital image processing, aims to improve image quality by highlighting desired elements and reducing obscuration.

This study provides an overview of the history and relevant research on Histogram Equalization (HE)-based image enhancement. HE is a simple method, and numerous adjustments have been published to optimize the normalization process. Future research on the mathematical algorithms in HE is warranted. Additionally, the study reviews current approaches, including HE, Global Histogram Equalization (GHE), Local Histogram Equalization (LHE), Adaptive Histogram Equalization (AHE), Brightness Preserving Bi-Histogram Equalization (BBHE), Dualistic Sub-Image Histogram Equalization (DSIHE), Contrast Limited Adaptive Histogram Equalization (CLAHE), Recursive Sub-Image Histogram Equalization (RSIHE), and Gamma Correction Adaptive Extreme Level Eliminating with Weighting Distribution (GCAELEWD). While these methods improve contrast and clarity, some have drawbacks, such as noise enhancement, blur, and lengthy processing times.

ACKNOWLEDGMENT

The authors thank Multimedia University for supporting this research. All datasets are available in the public domain at: <https://www.kaggle.com/datasets/noshintasnia/brain-stroke-prediction-ct-scan-image-dataset>

REFERENCES

- [1] G. E. Christensen, S. C. Joshi, and M. I. Miller, "Volumetric transformation of brain anatomy," *IEEE Transactions on Medical Imaging*, vol. 16, no. 6, pp. 864–877, 1997, doi: 10.1109/42.650882.
- [2] N. Senthilkumaran and J. Thimmiraja, "Histogram Equalization for Image Enhancement Using MRI Brain Images," *2014 World Congress on Computing and Communication Technologies*, Feb. 2014, doi:10.1109/wccct.2014.45.
- [3] M. Qiao et al., "CHearT: A Conditional Spatio-Temporal Generative Model for Cardiac Anatomy," *IEEE Transactions on Medical Imaging*, vol. 43, no. 3, pp. 1259–1269, Mar. 2024, doi:10.1109/tmi.2023.3331982.
- [4] T. Badriyah, N. Sakinah, I. Syarif, and D. R. Syarif, "Segmentation Stroke Objects based on CT Scan Image using Thresholding Method," *2019 First International Conference on Smart Technology & Urban Development (STUD)*, vol. 7, pp. 1–6, Dec. 2019, doi:10.1109/stud49732.2019.9018825.
- [5] P. Garg, P. Kumar, K. Shakya, D. Khurana, and S. Roy Chowdhury, "Detection of Brain Stroke using Electroencephalography (EEG)," *2019 13th International Conference on Sensing Technology (ICST)*, vol. 9, pp. 1–6, Dec. 2019, doi: 10.1109/icst46873.2019.9047678.
- [6] A. Biffi, "Risk Factors for Hemorrhagic Stroke," *Stroke Revisited: Hemorrhagic Stroke*, pp. 7–25, 2018, doi: 10.1007/978-981-10-1427-7_2.

- [7] C. Shih, W. Cheng-Chung Chu, and Y.-W. Chang, "The Causes Analysis of Ischemic Stroke Transformation into Hemorrhagic Stroke using PLS (partial Least Square)-GA and Swarm Algorithm," *2019 IEEE 43rd Annual Computer Software and Applications Conference (COMPSAC)*, vol. 48, pp. 720–729, Jul. 2019, doi:10.1109/compsac.2019.00108.
- [8] I. Grigore, G. Diaconu, A. Mania, and I. Ciomaga, "Ischemic stroke by multifactorial cause in children," *2017 E-Health and Bioengineering Conference (EHB)*, pp. 221–224, Jun. 2017, doi:10.1109/ehb.2017.7995401.
- [9] D. Ichwana, M. Arief, N. Puteri, and S. Ekariani, "Movements Monitoring and Falling Detection Systems for Transient Ischemic Attack Patients Using Accelerometer Based on Internet of Things," *2018 International Conference on Information Technology Systems and Innovation (ICITSI)*, Oct. 2018, doi: 10.1109/icitsi.2018.8695959.
- [10] R. A. Karnavat, E. B. Patole, A. S. Parkhi, M. A. Muluk, and S. J. More, "Stroktor-A System to Predict Ischemic Brain Stroke using Learning Techniques," *2023 3rd International Conference on Intelligent Technologies (CONIT)*, vol. 48, pp. 1–4, Jun. 2023, doi:10.1109/conit59222.2023.10205858.
- [11] L. Caplan, "Stroke Is Best Managed by Neurologists," *Stroke*, vol. 34, no. 11, pp. 2763–2763, Nov. 2003, doi:10.1161/01.str.0000099140.79571.88.
- [12] A. Hussain and A. Khunteta, "Semantic Segmentation of Brain Tumor from MRI Images and SVM Classification using GLCM Features," *2020 Second International Conference on Inventive Research in Computing Applications (ICIRCA)*, vol. 2, pp. 38–43, Jul. 2020, doi:10.1109/icirca48905.2020.9183385.
- [13] A. Wulandari, R. Sigit, and M. M. Bachtiar, "Brain Tumor Segmentation to Calculate Percentage Tumor Using MRI," *2018 International Electronics Symposium on Knowledge Creation and Intelligent Computing (IES-KCIC)*, Oct. 2018, doi:10.1109/kcic.2018.8628591.
- [14] C. C. Gaudes, P. A. Bandettini, and J. Gonzalez-Castillo, "A temporal deconvolution algorithm for multiecho functional MRI," *2018 IEEE 15th International Symposium on Biomedical Imaging (ISBI 2018)*, vol. 29, pp. 608–611, Apr. 2018, doi: 10.1109/isbi.2018.8363649.
- [15] A. Mansur, R. Newbould, G. E. Searle, C. Redstone, R. N. Gunn, and W. A. Hallett, "PET-MR Attenuation Correction in Dynamic Brain PET Using [11C]Cimbi-36: A Direct Comparison With PET-CT," *IEEE Transactions on Radiation and Plasma Medical Sciences*, vol. 2, no. 5, pp. 483–489, Sep. 2018, doi: 10.1109/trpms.2018.2852558.
- [16] J. P. Frizzell, "Acute Stroke," *AACN Clinical Issues: Advanced Practice in Acute and Critical Care*, vol. 16, no. 4, pp. 421–440, Oct. 2005, doi: 10.1097/00044067-200510000-00002.
- [17] M. Al-Biltagi, "Imaging of Congenital Subclavian Artery to Subclavian Vein Fistula in a Newborn," *Cardiology and Angiology: An International Journal*, vol. 2, no. 4, pp. 180–192, Jan. 2014, doi:10.9734/ca/2014/10845.
- [18] V. Nedel'ko, R. Kozinets, A. Tulupov, and V. Berikov, "Comparative Analysis of Deep Neural Network and Texture-Based Classifiers for Recognition of Acute Stroke using Non-Contrast CT Images," *2020 Ural Symposium on Biomedical Engineering, Radioelectronics and Information Technology (USBEREIT)*, vol. 11353, pp. 376–379, May 2020, doi: 10.1109/usberoit48449.2020.9117784.
- [19] A.-C. Phan, T.-M.-N. Nguyen, and T.-C. Phan, "Detection and Classification of Brain Hemorrhage Based on Hounsfield Values and Convolution Neural Network Technique," *2019 IEEE-RIVF International Conference on Computing and Communication Technologies (RIVF)*, vol. 1, pp. 1–7, Mar. 2019, doi:10.1109/rivf.2019.8713733.
- [20] Simply Radiology, "brain window," *Simply Radiology*, Sep. 02, 2017. <https://sugarytooth.wordpress.com/tag/brain-window/>.
- [21] T. L. Tan, K. S. Sim, and A. K. Chong, "Contrast enhancement of CT brain images for detection of ischemic stroke," *2012 International Conference on Biomedical Engineering (ICoBE)*, vol. 2008, pp. 385–388, Feb. 2012, doi: 10.1109/icobe.2012.6179043.
- [22] S. Fawaz, K. S. Sim, and S. C. Tan, "Encoding Rich Frequencies for Classification of Stroke Patients EEG Signals," *IEEE Access*, vol. 8, pp. 135811–135820, 2020, doi: 10.1109/access.2020.3011185.
- [23] C. K. Toa, K. S. Sim, and S. C. Tan, "Electroencephalogram-Based Attention Level Classification Using Convolution Attention Memory Neural Network," *IEEE Access*, vol. 9, pp. 58870–58881, 2021, doi:10.1109/access.2021.3072731.
- [24] K. S. Sim, S. C. Tan, and Y. Z. Lim, "An Evaluation of Left and Right Brain Dominance using Electroencephalogram Signal," *Engineering Letters*, vol. 28, no. 4, p. 1358, 2020.
- [25] V. Teh, K. S. Sim, and E. K. Wong, "Brain early infarct detection using gamma correction extreme-level eliminating with weighting distribution," *Scanning*, vol. 38, no. 6, pp. 842–856, Jun. 2016, doi:10.1002/sca.21334.
- [26] J. L. C. Loong, K. S. Sim, R. Bear, K. S. Subari, and M. K. Abdullah, "Effects of diseased ECG on the robustness of ECG biometric systems," *2010 IEEE EMBS Conference on Biomedical Engineering and Sciences (IECBES)*, pp. 307–310, Nov. 2010, doi:10.1109/iecbes.2010.5742250.
- [27] K. S. Sim, M. K. Ong, C. K. Tan, C. P. Tso, and A. H. Rozalina, "Early Ischemic Stroke Detection through Image Colorization Graphical User Interface," *5th Kuala Lumpur International Conference on Biomedical Engineering 2011*, pp. 639–642, 2011, doi: 10.1007/978-3-642-21729-6_157.
- [28] K. S. Sim and F. Sammani, "Deep Convolutional Networks for Magnification of Dicom Brain Images," *International Journal of Innovative Computing, Information and Control ICIC International*, vol. 15, no. 2, pp. 725–739, 2019.
- [29] K. S. Sim, M.K. Ong, S.S. Chong, JT Ng, C.P. Tso, S.L. Choo, A.H. Rozalina, "Auto detection of brain ventricles using Hausdorff distance," *2010 IEEE EMBS Conference on Biomedical Engineering and Sciences (IECBES)*, vol. 4, pp. 199–204, Nov. 2010, doi:10.1109/iecbes.2010.5742228.
- [30] C. J. Lew, K. S. Sim, and T. K. Kho, "Contrast and Brightness Enhancement for DICOM Images and Lesions Auto Detection," *Journal of Image and Graphics*, vol. 4, no. 1, pp. 25–28, 2016, doi:10.18178/joig.4.1.25-28.
- [31] N. C. Y. Koh, K. S. Sim, and C. P. Tso, "CT brain lesion detection through combination of recursive sub-image histogram equalization in wavelet domain and adaptive gamma correction with weighting distribution," *2016 International Conference on Robotics, Automation and Sciences (ICORAS)*, vol. 52, pp. 1–6, Nov. 2016, doi:10.1109/icoras.2016.7872603.
- [32] K. S. Sim, M. E. Nia, C. S. Ta, C. P. Tso, T. K. Kho, and C. S. Ee, "Evaluation of Window Parameters of CT Brain Images with Statistical Central Moments," *Emerging Trends in Applications and Infrastructures for Computational Biology, Bioinformatics, and Systems Biology*, pp. 493–503, 2016, doi: 10.1016/b978-0-12-804203-8.00032-8.
- [33] K. S. Sim, Z. Y. Lim and F. Sammani, "Development of Dementia Neurofeedback System Using EEG Brainwave Signals," *International Journal of Signal Processing Systems*, vol. 7, no. 4, pp. 113–117, Dec. 2019, doi: 10.18178/ijsp.7.4.113-117.
- [34] K.S. Sim, C.P. Tso, Y.Y. Tan, K.K. Law, A.B. J. Teoh, "Real-time image dynamic range compensation for an optical imaging system," *Journal of Electronic Imaging*, vol. 16, no. 3, p. 033006, Jul. 2007, doi:10.1117/1.2768964.
- [35] Z. Y. Lim, C. K. Toa, E. Rao, and K. S. Sim, "Development of Augmented Reality Based Applications for Brain Memory Training," *International Journal on Robotics, Automation and Sciences*, vol. 5, no. 1, pp. 13–20, Apr. 2023, doi:10.33093/ijoras.2023.5.1.3.
- [36] Z. Y. Lim, K. S. Sim, and S. C. Tan, "Metric Learning Based Convolutional Neural Network for Left-Right Brain Dominance Classification," *IEEE Access*, vol. 9, pp. 120551–120566, 2021, doi:10.1109/access.2021.3107554.
- [37] C. W. Ti, K. S. Sim, and F. S. Abas, "Contrast measurement for MRI images using histogram of second-order derivatives," *2017 International Conference on Robotics, Automation and Sciences (ICORAS)*, pp. 1–5, Nov. 2017, doi: 10.1109/icoras.2017.8308080.
- [38] K. S. Sim, S. E. Chung, and Y. L. Zheng, "Contrast Enhancement Brain Infarction Images Using Sigmoidal Eliminating Extreme Level Weight Distributed Histogram Equalization," *International Journal of Innovative Computing, Information and Control*, 2018, vol. 14, no. 3, pp. 1043–1056, 2018.
- [39] Z.Y. Lim, K.S. Sim, S.C. Tan, "Metric Learning Based Convolutional Neural Network for Left-Right Brain Dominance Classification," *IEEE Access*, vol 9, no 1, pp. 120551 – 120566, 2021, doi:10.1109/ACCESS.2021.3107554.
- [40] F. F. Ting, K. S. Sim, and C. P. Lim, "Case-control comparison brain lesion segmentation for early infarct detection," *Computerized Medical Imaging and Graphics*, vol. 69, pp. 82–95, Nov. 2018, doi:10.1016/j.compmedimag.2018.08.011.
- [41] K. S. Sim, W. Z. W. Ismail, L. W. Thong, W.K.Lim, and H. Y. Ting, "Contrast-Enhancement with Contrast-Stretching Dynamic Histogram-Equalization," *In Proceedings of the LASTED International Conference*, vol. 654, p. 022. 2009.

- [42] K. Chua, Z. Y. Lim, K. S. Sim, and S. C. Tan, "Development of Brain Balancing System for Left and Right Hemispheres," *International Journal on Robotics, Automation and Sciences*, vol. 3, pp. 1–7, Nov. 2021, doi: 10.33093/ijoras.2021.3.1.
- [43] R. K. Y. Chang, S. H. Lau, K. S. Sim, and M. S. M. Too, "Kinect-based framework for motor rehabilitation," *2016 International Conference on Robotics, Automation and Sciences (ICORAS)*, pp. 1–4, Nov. 2016, doi: 10.1109/icoras.2016.7872606.
- [44] C. C. Lim, K. S. Sim, and C. K. Toa, "Development of Visual-based Rehabilitation Using Sensors for Stroke Patient," *International Journal on Robotics, Automation and Sciences*, vol. 2, pp. 25–30, Oct. 2020, doi: 10.33093/ijoras.2020.2.4.
- [45] C. S. Ee, K. S. Sim, V. Teh, and F. F. Ting, "Estimation of window width setting for CT scan brain images using mean of greyscale level to standard deviation ratio," *2016 International Conference on Robotics, Automation and Sciences (ICORAS)*, pp. 1–6, Nov. 2016, doi:10.1109/icoras.2016.7872600.
- [46] K. S. Sankaran, A. S. Poyyamozi, S. S. Ali, and Y. Jennifer, "Automated Brain Tumor Detection Model Using Modified Intrinsic Extrema Pattern based Machine Learning Classifier," *2021 Fourth International Conference on Electrical, Computer and Communication Technologies (ICECCT)*, vol. 21, pp. 1–6, Sep. 2021, doi:10.1109/icecct52121.2021.9616764.
- [47] G. N. B. Bethel, T. V. Rajinikanth, and S. V. Raju, "An Improved Analysis of Heart MRI Images using the Morphological Operations," *2017 International Conference on Current Trends in Computer, Electrical, Electronics and Communication (CTCEEC)*, vol. 4, pp. 891–897, Sep. 2017, doi: 10.1109/ctceec.2017.8455050.
- [48] T. Rahman and Md. S. Islam, "Image Segmentation Based on Fuzzy C Means Clustering Algorithm and Morphological Reconstruction," *2021 International Conference on Information and Communication Technology for Sustainable Development (ICICT4SD)*, Feb. 2021, doi:10.1109/icict4sd50815.2021.9396873.
- [49] A. Medda and V. DeBrunner, "Color Image Quality Index Based on the UIQI," *2006 IEEE Southwest Symposium on Image Analysis and Interpretation*, vol. 5007, pp. 213–217, doi:10.1109/ssiai.2006.1633753.
- [50] K. Joshi, R. Yadav, and S. Allwadh, "PSNR and MSE based investigation of LSB," *2016 International Conference on Computational Techniques in Information and Communication Technologies (ICCTICT)*, pp. 280–285, Mar. 2016, doi:10.1109/icctict.2016.7514593.
- [51] X. Ma, X. Jiang, and D. Pan, "Performance validation and analysis for multi-method fusion based image quality metrics in a new image database," *China Communications*, vol. 16, no. 8, pp. 147–161, Aug. 2019, doi: 10.23919/jcc.2019.08.013.
- [52] A. Hore and D. Ziou, "Image Quality Metrics: PSNR vs. SSIM," *2010 20th International Conference on Pattern Recognition*, pp. 2366–2369, Aug. 2010, doi: 10.1109/icpr.2010.579.
- [53] H. Krishnan, A. A. Lakshmi, L. S. Anamika, C. H. Athira, P. V. Alaikha, and V. M. Manikandan, "A Novel Underwater Image Enhancement Technique using ResNet," *2020 IEEE 4th Conference on Information & Communication Technology (ICT)*, Dec. 2020, doi: 10.1109/cict51604.2020.9311926.
- [54] F. Lounoughi and M. Djendi, "Decision Feedback Equalizer based Affine Projection and Normalized Least Mean Square Algorithms," *2023 International Conference on Advances in Electronics, Control and Communication Systems (ICAEECS)*, Mar. 2023, doi:10.1109/icaeeecs56710.2023.10105130.
- [55] K. A. Teo; K. S. Sim; C. K. Toa; K. L. Lew, "Development of Virtual Reality-Based Left Brain System," *Journal of Informatics and Web Engineering*, vol 3, no 6, pp. 98–120, doi: 10.33093/jiwe.2024.3.3.6,
- [56] Y. T. Kim, "Contrast enhancement using brightness preserving bi-histogram equalization," *IEEE Transactions on Consumer Electronics*, vol. 43, no. 1, pp. 1–8, 1997, doi: 10.1109/30.580378.
- [57] J. J. How, S. C. Tan, and K. S. Liew, "Masked Face Recognition Attendance System Using A Modified Convolutional Neural Network," *International Journal on Robotics, Automation and Sciences*, 4, pp. 23–29, 2022, <https://doi.org/10.33093/ijoras.2022.4.4>
- [58] Z. Wang, E. P. Simoncelli, and A. C. Bovik, "Multiscale structural similarity for image quality assessment," *The Thirty-Seventh Asilomar Conference on Signals, Systems & Computers*, 2003, doi: 10.1109/acssc.2003.1292216.
- [59] J. Cai, S. Gu, and L. Zhang, "Learning a Deep Single Image Contrast Enhancer from Multi-Exposure Images," *IEEE Transactions on Image Processing*, vol. 27, no. 4, pp. 2049–2062, Apr. 2018, doi:10.1109/tip.2018.2794218.
- [60] S. S. Chong, K. S. Sim, and M. E. Nia, "Modified HL contrast enhancement technique for breast MR images," *2013 IEEE International Conference on Signal and Image Processing Applications*, pp. 360–364, Oct. 2013, doi:10.1109/icsipa.2013.6708033.
- [61] W. T. Chan, "Conditional Noise Filter for MRI Images with Revised Theory on Second-order Histograms," *International Journal on Robotics, Automation and Sciences*, vol. 3, pp. 25–32, Nov. 2021, doi:10.33093/ijoras.2021.3.5.
- [62] J.P. Cheng, S.C. Haw, "Mental Health Problems Prediction Using Machine Learning Techniques," *International Journal on Robotics, Automation and Sciences*, 5(2), pp.59–72, doi:10.33093/ijoras.2023.5.2.7
- [63] N. M. Loorutu, H. Yazid, and K. S. Ab Rahman, "Prostate Cancer Classification Based on Histopathological Images," *International Journal on Robotics, Automation and Sciences*, vol. 5, no. 2, pp. 43–53, Sep. 2023, doi: 10.33093/ijoras.2023.5.2.5.
- [64] W. X. Lim, C. K. Toa, and K. S. Sim, "The Application of Augmented Reality Platform for Chemistry Learning," *International Journal on Robotics, Automation and Sciences*, vol. 5, no. 2, pp. 101–110, Sep. 2023, doi: 10.33093/ijoras.2023.5.2.13.
- [65] W. T. Chan, "Review on Present-day Breast Cancer Detection Techniques," *International Journal on Robotics, Automation and Sciences*, vol. 6, no. 1, pp. 94–101, Apr. 2024, doi:10.33093/ijoras.2024.6.1.13.
- [66] P. Decazes, P. Hinault, O. Veresezan, S. Thureau, P. Gouel, and P. Vera, "Trimodality PET/CT/MRI and Radiotherapy: A Mini-Review," *Frontiers in Oncology*, vol. 10, Feb. 2021, doi:10.3389/fonc.2020.614008.
- [67] K. Woldendorp, B. Indja, P. G. Bannon, J. P. Fanning, B. T. Plunkett, and S. M. Grieve, "Silent brain infarcts and early cognitive outcomes after transcatheter aortic valve implantation: a systematic review and meta-analysis," *European Heart Journal*, vol. 42, no. 10, pp. 1004–1015, Feb. 2021, doi: 10.1093/eurheartj/ehab002.
- [68] K. Singh and R. Kapoor, "Image enhancement using Exposure based Sub Image Histogram Equalization," *Pattern Recognition Letters*, vol. 36, pp. 10–14, Jan. 2014, doi: 10.1016/j.patrec.2013.08.024.
- [69] X. Guo, Y. Li, and H. Ling, "LIME: Low-Light Image Enhancement via Illumination Map Estimation," *IEEE Transactions on Image Processing*, vol. 26, no. 2, pp. 982–993, Feb. 2017, doi:10.1109/tip.2016.2639450.
- [70] A. M. Reza, "Realization of the Contrast Limited Adaptive Histogram Equalization (CLAHE) for Real-Time Image Enhancement," *The Journal of VLSI Signal Processing-Systems for Signal, Image, and Video Technology*, vol. 38, no. 1, pp. 35–44, Aug. 2004, doi:10.1023/b:vlsi.0000028532.53893.82.
- [71] K. S. Sim, Y. Y. Tan, M. A. Lai, C. P. Tso, and W. K. Lim, "Reducing scanning electron microscope charging by using exponential contrast stretching technique on post-processing images," *Journal of Microscopy*, vol. 238, no. 1, pp. 44–56, Mar. 2010, doi:10.1111/j.1365-2818.2009.03328.x.
- [72] P. Brocken, H. F. M. van der Heijden, P. N. R. Dekhuijzen, L. Peters-Bax, and L.-F. de Geus-Oei, "High Performance of 18F-Fluorodeoxyglucose Positron Emission Tomography and Contrast-Enhanced CT in a Rapid Outpatient Diagnostic Program for Patients with Suspected Lung Cancer," *Respiration*, vol. 87, no. 1, pp. 32–37, Apr. 2013, doi: 10.1159/000347096.
- [73] R. J. McDonald et al., "Intracranial Gadolinium Deposition after Contrast-enhanced MR Imaging," *Radiology*, vol. 275, no. 3, pp. 772–782, Jun. 2015, doi: 10.1148/radiol.15150025.
- [74] F. Abuhourea, K.S. Sim, Y.C. Wong, "Multi-User Human Activity Recognition Through Adaptive Location-Independent WiFi Signal Characteristics," *IEEE Access*, vol 12, pp. 112008 – 112024, 2024, doi: 10.1109/ACCESS.2024.3438871
- [75] S Fawaz, K.S Sim, S.C Tan, "Encoding Rich Frequencies for Classification of Stroke Patients EEG Signals," *IEEE access*, vol 8, 2020, pp. 135811- 135820,
- [76] F. H. O. Alfadhli, A. A. Mand, Md. S. Sayeed, K. S. Sim, and M. Al-Shabi, "Classification of tuberculosis with SURF spatial pyramid features," *2017 International Conference on Robotics, Automation and Sciences (ICORAS)*, pp. 1–5, Nov. 2017, doi:10.1109/icoras.2017.8308044.